This article has been accepted for publication in a future issue of this journal, but has not been fully edited. Content may change prior to final publication. Citation information: DOI 10.1109/TBME.2017.2744667, IEEE Transactions on Biomedical Engineering

Molecularly Imprinted Polymer-Based Electrochemical Biosensor for Bone Loss Detection

Nasrin Afsarimanesh*, Subhas Chandra Mukhopadhyay, *Fellow, IEEE* and Marlena Kruger

***Abstract*— Serum C-terminal telopeptide of type I collagen (CTx-I) assays quantify the fragment of CTx-I released throughout the procedure of bone remodeling. CTx-I is a key bone turnover biomarker where any variation in the level of CTx-I can be an indication of increased bone resorption. This study focuses on a new strategy for the prognosis of bone loss by monitoring the concentration of CTx-I in serum. An interdigital capacitive sensor together with Electrochemical Impedance Spectroscopy (EIS) was employed to assess the dielectric properties of the test solution. Artificial antibodies have been prepared for CTx-I molecules using the molecular imprinting technique. The sensor was functionalized using the synthesized Molecular Imprinted Polymer (MIP) in order to introduce the selectivity of CTx-I biomarker to the sensor. Calibration experiments were performed using different known concentration of sample solutions. The proposed biosensor showed a good linear response between 0.1 and 2.5 ng/ml. The detection limit of 0.09 ng/ml was found, encompassing the normal reference ranges required for recognition of bone turnover. Unknown real serum samples obtained from sheep blood were analysed using the proposed biosensor. The validation of the suggested technique was done using enzyme-linked immunosorbent assay (ELISA). The developed biosensor exhibited a good correlation with ELISA.**

***Index Terms*—Osteoporosis, C-terminal telopeptide, Interdigital sensors, Electrochemical Impedance Spectroscopy, Molecular Imprinted Polymer.**

I. Introduction

BONE, as a living dynamic tissue is continuously remodeled throughout life. The remodeling process can be profoundly affected by the level of activity by osteoblasts and osteoclasts [1, 2]. In women, bone loss is very high in the first years after menopause and this is one of the main causes of developing osteoporosis [3, 4]. Under normal conditions, bone resorption and bone formation are coupled with each other to provide a balance in skeletal metabolism [5]. Osteoporosis usually develops when bone resorption occurs quicker than bone formation. The main component of the organic mass of bone is formed by type-I collagen. Throughout the phase of bone resorption, type-I collagen is deteriorated and small fragments of CTx-I is delivered into blood and urine [6]. Thus, it could be used as a biomarker that is able to measure the rate of bone loss [7]. A normal person 0.040 ng/ml- 0.630 ng/ml serum CTx-I, exceeding this level can be considered as an indication of increased bone loss [8].

During the recent years, investigation on the biochemical markers of bone turnover and the specific assays for detection has considerably increased [9]. Among the several available biomarkers, monitoring serum C-terminal telopeptides and urinary N-terminal and C-terminal telopeptides are the most precise biomarkers. Biochemical bone turnover markers can inform about the risk of osteoporotic fractures at very early stages of the disease. They can also monitor the efficacy of treatments and can be used as a tool for the investigation of patients with a bone health problem [5].

Dual-energy X-ray absorptiometry (DXA) is the most acurate method to dignose osteoporosis and measure the bone density. As variations in bone density are slow, DXA scan can be of longer intervals between the measurements, up to 2 years at least, while variations in biochemical markers can be observed after only a few weeks. Therefore, measurement of biochemical markers (especially CTx-I) can be done at early stages and treatment can start early. Currently, most of the techniques which are available for the measurement of bone loss biomarkers are ELISA-based [10-12]. In spite of the perfect performance, these methods have some limitations due to the high equipment cost and the labour involved. Moreover, these methods include several steps for antibody binding, incubation and spectrophotometry measurement. Devices that combine the use of antigen-antibody methods with a low-cost and quick-response sensor seems to be a good replacement for ELISA-based immunoassay techniques [13-15]. However, there are some drawbacks in using natural antibodies: antibody immobilization procedure is complicated, biological antibodies are expensive and have limited stability. Moreover, sample preparation is a complex and time-consuming process. Use of artificial antibodies can be greatly helpful to overcome these problems.

Molecular imprinting technology is a rapid and inexpensive technique to synthesize polymers that have selectivity and sensitivity to a predetermined molecule. The Molecularly Imprinted Polymers (MIPs) can be considered as a cost-effective substitute for natural antibodies. In this technique polymerization was done between the template and functional monomer using a cross-linker. After forming the polymer, the template molecules are extracted and molecular recognition cavities are created to capture the target molecule. The resultant polymer has superior mechanical as well as thermal stability

*N. Afsarimanesh and S. C. Mukhopadhyay are with the School of Engineering, Macquarie University, Sydney, NSW 2109, Australia. (e-mail: nasrin.afsarimanesh1@students.mq.edu.au;subhas.mukhopadhyay@mq.edu.au).

M. Kruger is with the School of Food and Nutrition, Massey University, Palmerston North, New Zealand (e-mail: m.c.kruger@massey.ac.nz).

This article has been accepted for publication in a future issue of this journal, but has not been fully edited. Content may change prior to final publication. Citation information: DOI 10.1109/TBME.2017.2744667, IEEE Transactions on Biomedical Engineering

and can be used in harsh chemical environments [16]. MIP technology has been utilized for a range of different template molecules [17-20]. MIPs have been successfully employed in different applications as solid phase extraction materials [21], binding assays [22, 23] and enzyme-mimic catalysts [24-26] and they are progressively being used in imprinted layers to develop chemical sensors [27, 28].

The use of MIPs has been reported for the development of electrochemical sensors depended on different transduction models such as conductometric [29], potentiometric [30], voltametric [31] and capacitive sensors [32]. Recently, the capacitive sensors have gained attraction because they provide sensitive, inexpensive and straightforward recognition methods [33-35].

The objective of this research is to design a smart biosensing system for early detection of bone loss that is easy to use, inexpensive, and quick and can be used as a Point-of-Care (POC) device outside the laboratories. Therefore, the development of a portable device that combines the advantages of MIP based **artificial** antibodies with a fast and inexpensive electrochemical sensor seems to be a very promising approach towards our goal.

As per our knowledge, so far, no MIP-based interdigital sensor has been introduced for CTx-I detection. This paper explains the development of a capacitive CTx-I biosensor by combining MIP technology and EIS technique for a sensitive and rapid measurement of serum CTx-I.

II. Materials and Methods

A. Materials and Apparatus

CTx-I peptide was synthesized by LifeTein (USA). Methacrylic acid (MAA), 2,2-azoisobutronitrile (AIBN), ethylene glycol methacrylate (EGDMA), acetonitrile (ACN), Methanol (MeOH), Acetic acid (AcOH), and acrylic resin were purchased from Sigma-Aldrich (USA).

High precision 3536 LCR meter (Hioki, Japan) was employed to conduct EIS experiments. SIGMA 6-165 centrifuge instrument was used during the preparation of MIP. DIONEX Ultimate 3000 HPLC device provided with Luna 5µ C18 100A column and the Serum CrossLaps® ELISA kit (IDS company-UK) were employed for data validation. JEOL 6480LA SEM was utilized to take SEM images and PTL-MM01 dip coater was employed to immobilize the coating material on the sensing area.

B. Multi-sensing electrode interdigital sensor and electrochemical impedance spectroscopy

Capacitive sensing method is significantly affected by the double layer capacitance principle and any adsorption of chemicals on the dielectric material leads to a variation in the dielectric properties of the insulating layer.

In the reported research, capacitive interdigital sensors with multi-sensing electrode structure were used. The MEMS-based sensors are useful to describe the capacitive reactance when alternating electric field perturbations are applied. The electric field penetrates into the test material to conduct the dielectric characterization of the material. In interdigital sensors, the penetration depth of electric field is corresponding to the spatial wavelength of the interdigital sensor [36, 37]. To enhance the penetration depth, planar interdigital sensors with multi-sensing electrodes have been designed and fabricated [38]. These sensors were fabricated on a 4-inch silicon wafer (525-µm thickness). Thirty-six good sensors with 500 nm sputtered gold electrodes were made on a wafer; the dimension of each sensor is 10 mm × 10 mm with a sensing surface of 2.5 mm × 2.5 mm. The multi-sensing-electrode capacitive sensors have been designed with different configurations [39, 40]. The 1-11-50 sensor was employed to conduct the experiments, which shows eleven positive electrodes are located between two positive electrodes with a 50-µm pitch length.

EIS is a versatile method that describes the capacitive and resistive characteristics of materials by using a frequency dependent small amplitude AC signal [41]. The Bode plot and Nyquist plot are two common ways to represent the results of EIS measurement. Due to the high sensitivity and simplicity of the technique, it has been widely implemented in biosensor applications using different methods [42].

Interdigital sensors in conjunction with the EIS measurement method has been reported to evaluate the environmental monitoring [43], detection of phthalates in juices and water [44], dangerous chemicals in seafood [45], humidity [46] and DNA detection [47].

C. Preparation of artificial antibodies using molecular imprinting technology

A selective polymer for CTx-I was synthesized by precipitation polymerization using MAA as the functional monomer, CTx-I peptide as the template, AIBN as the initiator and EGDMA as the cross-linker.

A mixture was prepared by dissolving 450 mg of the template molecule (CTx-I) in 50 ml acetonitrile in a 150 ml round bottom flask, and then adding 260 µl of the functional monomer MAA, 3 ml of the cross-linker EGDMA, and 120 mg of the initiator. The N_2 gas was blown for 10 minutes to evacuate the air completely from the solution since the presence of oxygen hampers the polymerization procedure [48, 49]. The sealed flask was then kept in a 60˚C water bath for 20 hours to complete the polymerization process. The microspheres were collected by centrifugation for 10 minutes at 5000 rpm and then washed with acetonitrile to eliminate any excess peptides and chemicals. The extraction of the template was done using the Soxhlet extraction method with a mix of methanol/acetic acid 50/50 (v/v) for 24 hours. The non-imprinted polymer (NIP) was also prepared using the same method but in the absence of the template molecule. The NIP and MIP were air dried at room temperature and used for the experiments.

This article has been accepted for publication in a future issue of this journal, but has not been fully edited. Content may change prior to final publication. Citation information: DOI 10.1109/TBME.2017.2744667, IEEE Transactions on Biomedical Engineering

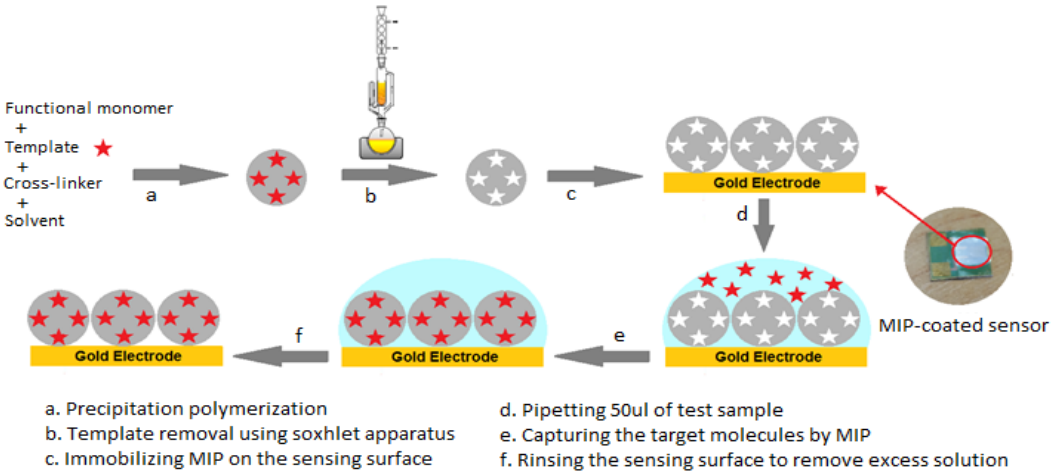

Fig. 1. Schematic diagram of the biosensing surface preparation for CTx-I recognition.

D. *Preparation of the functionalized biosensing surface*

The MIP coating material was immobilized on the biosensing area of the interdigital sensor using a self-assembled monolayer (SAM) of the acrylic resin. 1g of MIP powder, 200 µl of the acrylic resin and 1.5 ml of acetone were mixed together to prepare the coating suspension. The sensor was immersed into the coating material with a speed of 200 mm/min and pulled out with the same speed to create a uniform layer. The sensor was immersed into the coating material and pulled out with a speed of 200 mm/min to create a uniform layer. Fig. 1 is the illustrative representation of the biosensing surface preparation. It also depicts the detection procedure of the target molecule using the developed biosensor.

E. *Preparation of the CTx-I samples*

A stock solution of 60 ppm CTx-I was prepared by mixing 60 mg of CTx-I in one liter deionized water and it was kept in the fridge for further use. Serial dilution technique was utilized to prepare the samples with lower concentrations. The distilled water with zero level of CTx-I was treated as the control.

F. *Experimental measurements*

EIS technique was used to investigate the dielectric properties of the test samples at different concentrations. Although this measurement technique is very powerful and popular, it is really sensitive to humidity and temperature. Therefore, all the experiments were conducted in a controlled laboratory under the same humidity and temperature level. The coated sensor was connected to the LCR meter using gold pin connectors and a 10 Hz- 100 kHz signal with 1V amplitude was given to the electrodes. After pipetting the test sample (50 µl) on the MIP-coated area, the sensor was kept on a shaking plate for 30 seconds to ensure the uniform dispersion of the sample. Then, a seven minutes' delay was given for capturing CTx-I molecules by MIP. The extra solution was then washed out using deionized water. Finally, EIS measurement was done after five minutes, when the coating surface was dried. The sensor was immersed in 1% HCL in distilled water for 30 minutes to extract the entrapped CTx-I molecules and regenerate the functionalized MIP coating.

III. Results and Discussions

CTx-I imprinted polymer was synthesized through precipitation polymerization method, privileged by advantages such as high selectivity, robustness and physiochemical stability. In the pre-polymerization process, the template molecule interacted with the functional monomers through the non-covalent binding and during the polymerization procedure they were properly imprinted in the polymer matrix. The non-covalent method is more popular because it involves less effort to take out the template from the polymer matrix, while covalent bonding needs more energy to extract the template from the polymer. Furthermore, the prepared MIP can be used immediately after template extraction, whereas MIPs synthesized through bulk polymerization are required to be crushed and ground before use.

A. *SEM characterization*

After preparing the imprinted polymer in the form of microbeads and immobilizing the resultant polymer on the sensing area, SEM images were provided to study the polymer morphological structure as shown in Fig. 2(a). It was observed that the size of the particles was variable from 0.5 µm to 1µm. Moreover, MIP coating with an average thickness of 16 µm could be achieved on the biosensing surface, which can be seen in Fig. 2(b).

This article has been accepted for publication in a future issue of this journal, but has not been fully edited. Content may change prior to final publication. Citation information: DOI 10.1109/TBME.2017.2744667, IEEE Transactions on Biomedical Engineering

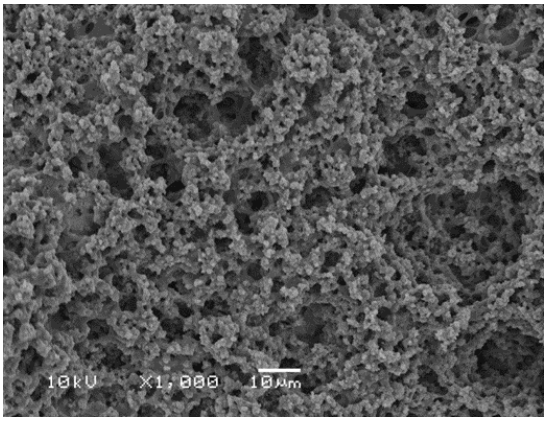

(a)

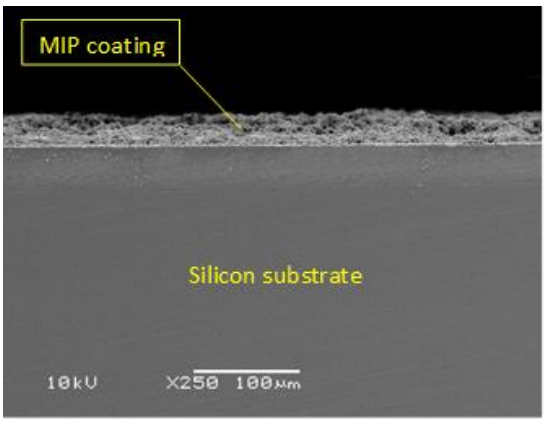

(b)

Fig. 2. (a) SEM image of MIP-coated biosensing surface and (b) SEM image of the MIP-coated sensor to show the thickness of the coating.

B. *Sorption studies of CTx-I to MIP and NIP*

The adsorption characteristics of the synthesized microbeads were inspected by HPLC analysis. DIONIX HPLC device equipped with Luna C18 column was used to determine the amount of CTx-I molecules entrapped by the polymer. Two different solutions were prepared for the mobile phase. Solution A contained 0.1% trifluoroacetic acid in acetonitrile and solution B was prepared by mixing 0.1% trifluoroacetic acid in water. The isocratic elution was performed for 25 min with a mobile phase configuration of 26% A and 74% B. The flow rate was kept at 1 ml/min. The injection volume was set at 100 µl and the detection was done at λ=220 nm.

The static adsorption capacity of the polymer was calculated using (1):

$$Q = \frac{V(C_i - C_f)}{m} \qquad (1)$$

Where Q (mg g-1) is the mass of CTx-I adsorbed per gram of polymer, V (l) is the total volume of the adsorption solution. Ci (mg.l-1) and Cf (mg.l-1) are the initial and final concentrations of CTx-I, respectively and m (g) is the mass of the polymer.

The kinetic studies were useful to estimate the time required by the polymer to entrap the CTx-I molecules present in the sample. This study was carried on by mixing 10 mg of MIP in 10 ml of CTx-I sample with the concentration of 30 mg.l-1.

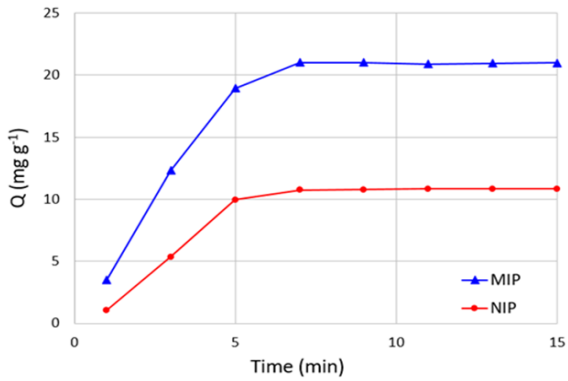

(a)

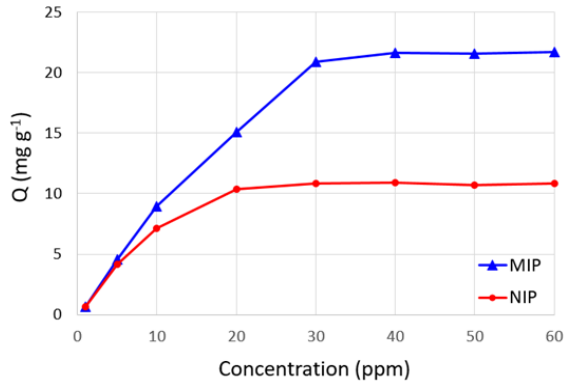

(b)

Fig. 3. (a) Uptake kinetics of CTx-I to MIP and NIP, and (b) Isotherms for static adsorption capacity of CTx-I to MIP and NIP.

Fig. 3(a) represents the results for the adsorption kinetics of CTx-I to MIP and NIP. The results indicate that the MIP had a rapid response and the binding equilibrium was observed in 7 minutes. Fig. 3(b) depicts the static absorption study of the target molecule to NIP as well as MIP in a range of 1-60 mg.l-1. The graph indicates the amount of CTx-I captured by the polymer, which increased along with the increase in the level of CTx-I below 30 mg l-1. The adsorption capacity graph became relatively parallel to the concentration axis and saturated at high concentration. However, the amount of CTx-I bound to NIP reached saturation at only 20 mg l-1.

C. *EIS measurement and analytical measurement*

The detection of CTx-I binding to the synthesized recognition sites was determined using EIS technique. Fig. 4(a) depicts the impedance spectra for various levels of analyte in the form of a Nyquist plot. A significant decrease in the semicircle diameter could be seen, confirming the CTx-MIP interaction on the electrode surface caused a reduction in the charge transfer resistance (R_{ct}). Fig. 4(b) shows the reactance (X) over 10 Hz to 100 kHz frequency, for various CTx-I levels. Since changes in the reactance are more distinctive than the real part of the impedance (resistance), the reactance was considered for further investigations.

This article has been accepted for publication in a future issue of this journal, but has not been fully edited. Content may change prior to final publication. Citation information: DOI 10.1109/TBME.2017.2744667, IEEE Transactions on Biomedical Engineering

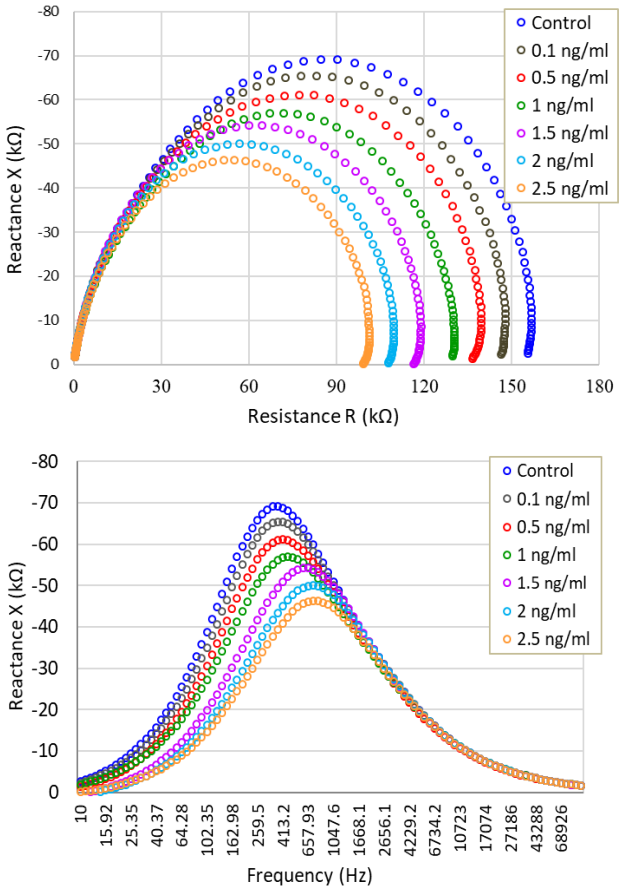

Fig. 4. (a) Impedance spectra for various levels of analyte, and (b) Changes in reactance in the frequency domain for various levels of analyte.

In order to assure the reliability of the sensor, each measurement was done three times in the identical conditions, and the mean value was considered as the data. Fig. 5 shows reactance values for each reading and the mean value of the reactance for different concentrations. The maximum deviation observed from the mean value was 0.5%, which demonstrates the consistency of the proposed biosensor.

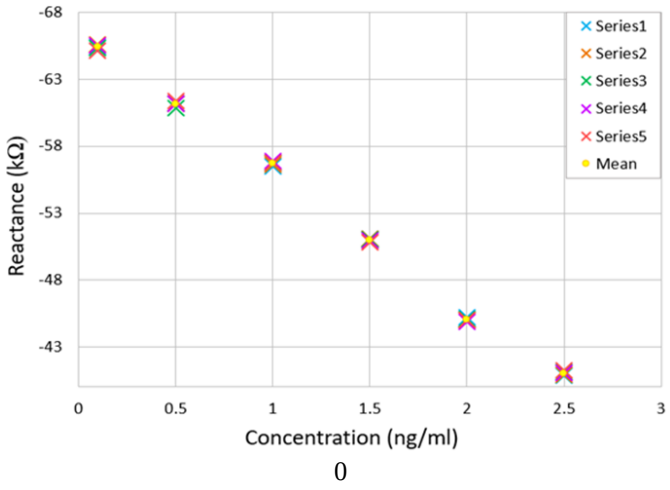

Fig. 5. Reactance value for five times reading to show the consistency of the biosensor.

D. *CNLS–based biosensor response*

Fig. 6 shows the Nyquist plot and its corresponding Randle's circuit estimated by using the CNLS technique [36]. The red markers on the graph illustrate the obtained results by experiment and the green line indicates the CNLS-fitted curve. The observed semicircle of the Nyquist plot is modeled using a parallel sketch of R_{ct} and a constant phase element (CPE). The solution resistance is represented by R_s.

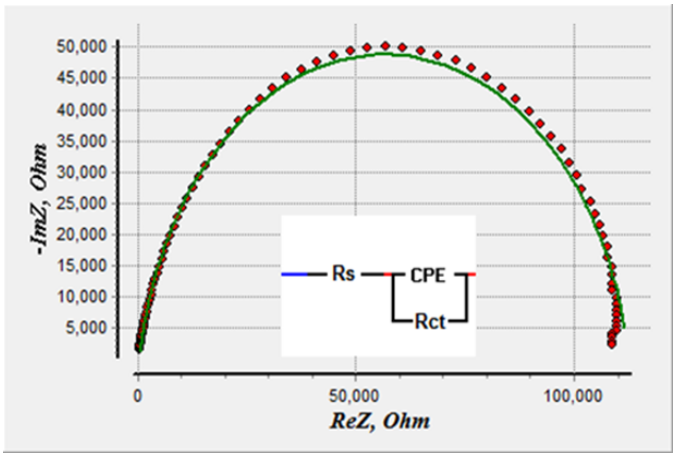

Fig. 6. The Nyquist plot and its corresponding Randle's model estimated by CNLS analysis.

The equivalent circuit parameters for different concentrations of analyte are provided in Table I, where $r^2_{amplitude}$ represents the variation of the experimentally obtained values from the optimum value. From Table I, it is seen that the charge transfer resistance, R_{ct} provides a very good relationship with the concentration of CTx-I. Therefore, the CNLS-based calibration curve can be plotted with the R_{ct} obtained from CNLS analysis and the following equation can be used to compute the change in R_{ct}:

$$\frac{\Delta R_{ct}}{R_{ct0}}(\%) = \frac{R_{ct}(control) - R_{ct}(sample)}{R_{ct}(control)} \times 100 \qquad (2)$$

Fig. 7(a) presents the CNLS-based calibration curve generated for 0.1 , 0.5 , 1, 1.5, 2 and 2.5 ng/ml of CTx-I. A linear correlation between the R_{ct} and the level of CTx-I was observed (R^2= 0.9953).

E. *Measurement of CTx-I in real serum samples using the CNLS–based calibration curve*

Sheep serum samples were tested using the developed biosensor as well as the ELISA kit for the validation of the proposed technique. CTx-I quantification in Real samples was done using the CNLS-based calibration curve (shown in Fig. 7(a)). The accuracy of the CTx-I quantification was examined by comparing the results achieved by the developed system with those achieved from the ELISA kit. All the results are given in Table II. The results achieved from both methods were in good agreement.

This article has been accepted for publication in a future issue of this journal, but has not been fully edited. Content may change prior to final publication. Citation information: DOI 10.1109/TBME.2017.2744667, IEEE Transactions on Biomedical Engineering

TABLE I
EQUIVALENT CIRCUIT PARAMETERS FOR DIFFERENT CTX-I CONCENTRATIONS

Component parameters	Control	0.1 ng/ml	0.5 ng/ml	1 ng/ml	1.5 ng/ml	2 ng/ml	2.5 ng/ml
R_s (Ω)	349.05	342.58	279.88	316.74	307.99	276.46	294.75
R_{ct} (kΩ)	163.3	154.4	144.6	135.3	121.9	112.3	104.2
CPE1(E-09)	6.356	6.463	6.750	5.986	4.181	3.998	4.324
$r^2_{amplitude}$	0.0029	0.0029	0.0024	0.0026	0.0016	0.0015	0.0015

TABLE II
DETERMINATION OF CTX-I CONCENTRATION IN REAL SERUM SAMPLES USING THE **CNLS–BASED CALIBRATION CURVE**

Sample	CTx-I level (ng/ml)		Error (%)
	Proposed sensor	Reference method ELISA	
S1	1.416	1.465	3.3
S2	0.184	0.187	1.6
S3	0.098	0.100	2.0
S4	0.453	0.450	0.6

TABLE III
DETERMINATION OF CTX-I CONCENTRATION IN REAL SERUM SAMPLES USING THE **SINGLE-FREQUENCY CALIBRATION CURVE**

Sample	CTx-I level (ng/ml)		Error (%)
	Proposed sensor	Reference method ELISA	
S1	1.416	1.465	3.3
S2	0.184	0.187	1.6
S3	0.098	0.100	2.0
S4	0.453	0.450	0.6

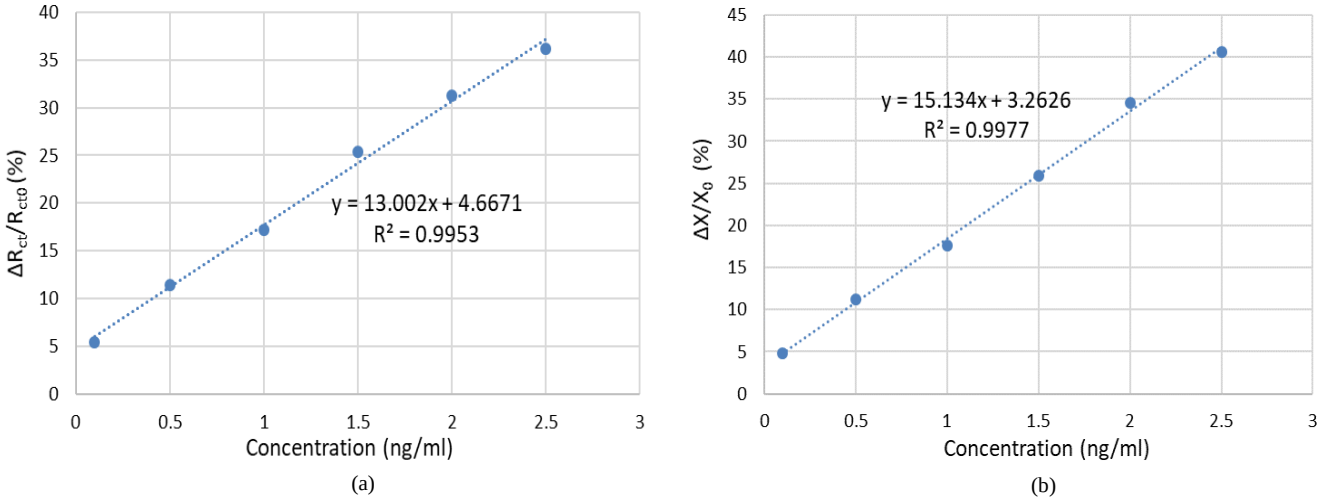

Fig. 7. (a) CNLS –based calibration curve representing change in R_{ct} to various concentrations of CTx-I, and (b) Single-frequency reactance-based calibration curve representing change in reactance (X) to various concentrations of CTx-I measured at 319 Hz.

This article has been accepted for publication in a future issue of this journal, but has not been fully edited. Content may change prior to final publication. Citation information: DOI 10.1109/TBME.2017.2744667, IEEE Transactions on Biomedical Engineering

F. Single-frequency reactance –based biosensor response

The proposed biosensor has a great potential to be used as a POC device for prognosis of bone turnover. Narrowing the frequency range to a single frequency makes data analysis more straightforward and efficient. It also reduces the total experimentation time. Therefore, the frequency of 319 Hz was determined as the optimum frequency according to the Nyquist analysis and changes in the reactance values. The percent change in reactance was then calculated at 319 Hz using the equation below:

$$\frac{\Delta X}{X_0}(\%) = \frac{X\,(control) - X\,(sample)}{X\,(control)} \times 100 \qquad (3)$$

The single-frequency reactance-based biosensor response is displayed in Fig. 7(b). It depicts the change in reactance for various concentrations of CTx-I (0.1 -2.5 ng/ml) at 319 Hz. There was a linear relationship between the reactance and the level of CTx-I with 0.9977 correlation coefficient.

G. Measurement of CTx-I in real serum samples using single-frequency based calibration curve

After developing the single-frequency calibration curve (Fig. 7(b)), the CTx-I quantification in sheep serum samples was performed using the developed calibration curve. The accuracy of the biosensor response was then compared with the ELISA response and the result of the comparison was presented as the percentage error in Table III.

H. Comparison between the CNLS-based measurement and single-frequency measurement

By comparing the results provided in Tables I and II, it can be observed that the CNLS-based testing can give more accurate results, as the measurement would be done in a wide range of frequencies. Moreover, the R_{ct} parameter is obtained from the theoretical fits and CNLS analysis. However, there are some significant advantages in implementing the single-frequency measurement, which are very useful in developing a portable POC device. The main privilege of using the single-frequency based measurement is that CNLS analysis is not required to derive the R_{ct} value. This would considerably minimize the actual measurement time for the biosensor and simplify the testing procedure. Therefore, the single-frequency measurement would be highly preferred as a sensing system, as it can offer a straightforward measurement approach and reduce the response time, which are predominant features in developing a quick and simple POC device.

IV. Conclusion

A novel sensing technique for the recognition of CTx-I by combining electrochemical impedance spectroscopy and MIP technology was introduced in this paper. The experiments were conducted on real serum samples. The proposed biosensor exhibited good selectivity and quick rebinding capacity towards target molecule. 0.09 ng/ml was the lowest level that could be detected by the developed biosensor. The limit of detection (LOD) obtained using the standard technique ELISA is 0.02 ng/ml, which is indeed less than the LOD obtained from the developed biosensor. However, at this stage, it should be noted that the proposed biosensing method represents a much simpler, quicker and more cost effective CTx-I detection technique. Moreover, the use of artificial antibodies highly improves the stability of the system. Therefore, the results demonstrate the potential of the developed biosensing system to be employed as a POC device for prognostic applications that can be utilized for a user-friendly and regular assessment of bone loss. Work is being done to associate the biosensor with an embedded system in order to develop a home testing kit in the near future.

Acknowledgment

We would like to thank Macquarie University microscopy unit, Faculty of Science and Engineering for the assistance by providing the SEM images. We are also grateful to Diana Cabrera Amaro, Massey University for her support and care during sample collection.

References

[1] A. G. Robling, A. B. Castillo, and C. H. Turner, "Biomechanical and molecular regulation of bone remodeling," *Annu. Rev. Biomed. Eng.*, vol. 8, pp. 455-498, 2006.

[2] D. J. Hadjidakis and I. I. Androulakis, "Bone remodeling," *Annals of the New York Academy of Sciences*, vol. 1092, pp. 385-396, 2006.

[3] D. M. Black and C. J. Rosen, "Postmenopausal osteoporosis," *New England Journal of Medicine*, vol. 374, pp. 254-262, 2016.

[4] J. Kanis, E. McCloskey, H. Johansson, C. Cooper, R. Rizzoli, and J.-Y. Reginster, "European guidance for the diagnosis and management of osteoporosis in postmenopausal women," *Osteoporosis international*, vol. 24, pp. 23-57, 2013.

[5] M. J. Seibel, S. P. Robins, and J. P. Bilezikian, *Dynamics of bone and cartilage metabolism: principles and clinical applications*: Academic Press, 2006.

[6] A. Srivastava, G. MacFarlane, V. Srivastava, S. Mohan, and D. Baylink, "A new monoclonal antibody ELISA for detection and characterization of C-telopeptide fragments of type I collagen in urine," *Calcified tissue international*, vol. 69, pp. 327-336, 2001.

[7] B. Lentle, A. M. Cheung, D. A. Hanley, W. D. Leslie, D. Lyons, A. Papaioannou, *et al.*, "Osteoporosis Canada 2010 guidelines for the assessment of fracture risk," *Canadian Association of Radiologists Journal*, vol. 62, pp. 243-250, 2011.

[8] S. Christgau, O. Bitsch-Jensen, N. H. Bjarnason, E. G. Henriksen, P. Qvist, P. Alexandersen, *et al.*, "Serum CrossLaps for monitoring the response in individuals undergoing antiresorptive therapy," *Bone*, vol. 26, pp. 505-511, 2000.

[9] P. Garnero, "New developments in biological markers of bone metabolism in osteoporosis," *Bone*, vol. 66, pp. 46-55, 2014.

[10] P. M. Crofton, N. Evans, M. R. Taylor, and C. V. Holland, "Serum CrossLaps: pediatric reference intervals from birth to 19 years of age," *Clinical chemistry*, vol. 48, pp. 671-673, 2002.

[11] C. Rosenquist, C. Fledelius, S. Christgau, B. J. Pedersen, M. Bonde, P. Qvist, *et al.*, "Serum CrossLaps One Step ELISA. First application of monoclonal antibodies for measurement in serum of bone-related degradation products from C-terminal telopeptides of type I collagen," *Clinical chemistry*, vol. 44, pp. 2281-2289, 1998.

[12] A. Claudon, P. Vergnaud, C. Valverde, A. Mayr, U. Klause, and P. Garnero, "New automated multiplex assay for bone turnover markers in osteoporosis," *Clinical chemistry*, vol. 54, pp. 1554-1563, 2008.

[13] N. Afsarimanesh, A. I. Zia, S. C. Mukhopadhyay, M. Kruger, P.-L. Yu, J. Kosel, *et al.*, "Smart Sensing System for the Prognostic Monitoring of Bone Health," *Sensors*, vol. 16, p. 976, 2016.

[14] Y.-H. Yun, A. Bhattacharya, N. B. Watts, and M. J. Schulz, "A label-free electronic biosensor for detection of bone turnover markers," *Sensors*, vol. 9, pp. 7957-7969, 2009.

[15] M. Ramanathan, M. Patil, R. Epur, Y. Yun, V. Shanov, M. Schulz, *et al.*, "Gold-coated carbon nanotube electrode arrays: Immunosensors for impedimetric detection of bone biomarkers," *Biosensors and Bioelectronics*, vol. 77, pp. 580-588, 2016.

[16] D. Kriz and K. Mosbach, "Competitive amperometric morphine sensor based on an agarose immobilised molecularly imprinted polymer," *Analytica chimica acta*, vol. 300, pp. 71-75, 1995.

[17] L. D. Bolisay, J. N. Culver, and P. Kofinas, "Molecularly imprinted polymers for tobacco mosaic virus recognition," *Biomaterials*, vol. 27, pp. 4165-4168, 2006.

[18] F. Trotta, E. Drioli, C. Baggiani, and D. Lacopo, "Molecular imprinted polymeric membrane for naringin recognition," *Journal of membrane science*, vol. 201, pp. 77-84, 2002.

[19] M. Odabaşi, R. Say, and A. Denizli, "Molecular imprinted particles for lysozyme purification," *Materials Science and Engineering: C*, vol. 27, pp. 90-99, 2007.

[20] H. Huo, H. Su, and T. Tan, "Adsorption of Ag+ by a surface molecular-imprinted biosorbent," *Chemical Engineering Journal*, vol. 150, pp. 139-144, 2009.

[21] B. Sellergren, "Direct drug determination by selective sample enrichment on an imprinted polymer," *Analytical chemistry*, vol. 66, pp. 1578-1582, 1994.

[22] L. Ye and K. Haupt, "Molecularly imprinted polymers as antibody and receptor mimics for assays, sensors and drug discovery," *Analytical and bioanalytical chemistry*, vol. 378, pp. 1887-1897, 2004.

[23] G. Vlatakis, L. I. Andersson, R. Müller, and K. Mosbach, "Drug assay using antibody mimics made by molecular imprinting," 1993.

[24] T. Takeuchi, T. Mukawa, J. Matsui, M. Higashi, and K. D. Shimizu, "Molecularly imprinted polymers with metalloporphyrin-based molecular recognition sites coassembled with methacrylic acid," *Analytical chemistry*, vol. 73, pp. 3869-3874, 2001.

[25] P. T. Vallano and V. T. Remcho, "Affinity screening by packed capillary high-performance liquid chromatography using molecular imprinted sorbents: I. Demonstration of feasibility," *Journal of Chromatography A*, vol. 888, pp. 23-34, 2000.

[26] Y. Li, Q. Ma, Z. Liu, X. Wang, and X. Su, "A novel enzyme-mimic nanosensor based on quantum dot-Au nanoparticle@ silica mesoporous microsphere for the detection of glucose," *Analytica chimica acta*, vol. 840, pp. 68-74, 2014.

[27] A. Ersöz, V. G. Gavalas, and L. G. Bachas, "Potentiometric behavior of electrodes based on overoxidized polypyrrole films," *Analytical and bioanalytical chemistry*, vol. 372, pp. 786-790, 2002.

[28] E. Hedborg, F. Winquist, I. Lundström, L. I. Andersson, and K. Mosbach, "Some studies of molecularly-imprinted polymer membranes in combination with field-effect devices," *Sensors and actuators A: Physical*, vol. 37, pp. 796-799, 1993.

[29] T. áL Panasyuk and L. áM Sergeeva, "Conductimetric sensor for atrazine detection based on molecularly imprinted polymer membranes," *Analyst*, vol. 124, pp. 331-334, 1999.

[30] C. Malitesta, I. Losito, and P. G. Zambonin, "Molecularly imprinted electrosynthesized polymers: new materials for biomimetic sensors," *Analytical Chemistry*, vol. 71, pp. 1366-1370, 1999.

[31] P. Andrea and M. Stanislav, "A solid binding matrix/molecularly imprinted polymer-based sensor system for the determination of clenbuterol in bovine liver using differential-pulse voltammetry," *Sensors and Actuators B: Chemical*, vol. 76, pp. 286-294, 2001.

[32] Z. Cheng, E. Wang, and X. Yang, "Capacitive detection of glucose using molecularly imprinted polymers," *Biosensors and Bioelectronics*, vol. 16, pp. 179-185, 2001.

[33] L. Yang, W. Wei, J. Xia, H. Tao, and P. Yang, "Capacitive biosensor for glutathione detection based on electropolymerized molecularly imprinted polymer and kinetic investigation of the recognition process," *Electroanalysis*, vol. 17, pp. 969-977, 2005.

[34] F. Yin, "Capacitive sensors using electropolymerized o-phenylenediamine film doped with ion-pair complex as selective elements for the determination of pentoxyverine," *Talanta*, vol. 63, pp. 641-646, 2004.

[35] A. Aghaei, M. R. M. Hosseini, and M. Najafi, "A novel capacitive biosensor for cholesterol assay that uses an electropolymerized molecularly imprinted polymer," *Electrochimica acta*, vol. 55, pp. 1503-1508, 2010.

[36] A. V. Mamishev, K. Sundara-Rajan, Y. Fumin, D. Yanqing, and M. Zahn, "Interdigital sensors and transducers," *Proceedings of the IEEE*, vol. 92, pp. 808-845, 2004.

[37] A. V. Mamishev, Y. Du, J. H. Bau, B. C. Lesieutre, and M. Zahn, "Evaluation of diffusion-driven material property profiles using three-wavelength interdigital sensor," *IEEE Transactions on Dielectrics and Electrical Insulation*, vol. 8, pp. 785-798, 2001.

[38] A. I. Zia, M. S. A. Rahman, S. C. Mukhopadhyay, P.-L. Yu, I. H. Al-Bahadly, C. P. Gooneratne, *et al.*, "Technique for rapid detection of phthalates in water and beverages," *Journal of Food Engineering*, vol. 116, pp. 515-523, 2013.

[39] A. M. Syaifudin, M. Yunus, S. Mukhopadhyay, and K. Jayasundera, "A novel planar interdigital sensor for environmental monitoring," in *Sensors, 2009 IEEE*, 2009, pp. 105-110.

[40] A. M. Syaifudin, K. Jayasundera, and S. Mukhopadhyay, "A low cost novel sensing system for detection of dangerous marine biotoxins in seafood," *Sensors and Actuators B: Chemical*, vol. 137, pp. 67-75, 2009.

[41] H. Wang and L. Pilon, "Intrinsic limitations of impedance measurements in determining electric double layer capacitances," *Electrochimica Acta*, vol. 63, pp. 55-63, 2012.

[42] E. P. Randviir and C. E. Banks, "Electrochemical impedance spectroscopy: an overview of bioanalytical applications," *Analytical Methods*, vol. 5, pp. 1098-1115, 2013.

[43] M. E. E. Alahi, X. Li, S. Mukhopadhyay, and L. Burkitt, "A Temperature Compensated Smart Nitrate-Sensor for Agricultural Industry," *IEEE Transactions on Industrial Electronics*, 2017.

[44] A. I. Zia, S. C. Mukhopadhyay, P.-L. Yu, I. H. Al-Bahadly, C. P. Gooneratne, and J. Kosel, "Rapid and molecular selective electrochemical sensing of phthalates in aqueous solution," *Biosensors and Bioelectronics*, vol. 67, pp. 342-349, 2015.

[45] A. M. Syaifudin, K. Jayasundera, and S. Mukhopadhyay, "A novel planar interdigital sensor based sensing and instrumentation for detection of dangerous contaminated chemical in seafood," in *Instrumentation and Measurement Technology Conference, 2009. I2MTC'09. IEEE*, 2009, pp. 701-706.

[46] T. Islam, Z. U. Rahman, and S. C. Mukhopadhyay, "A novel sol–gel thin-film constant phase sensor for high humidity measurement in the range of 50%–100% RH," *IEEE Sensors Journal*, vol. 15, pp. 2370-2376, 2015.

[47] T. Ramulu, R. Venu, B. Sinha, B. Lim, S. Jeon, S. Yoon, *et al.*, "Nanowires array modified electrode for enhanced electrochemical detection of nucleic acid," *Biosensors and Bioelectronics*, vol. 40, pp. 258-264, 2013.

[48] A. Ersöz, A. Denizli, A. Özcan, and R. Say, "Molecularly imprinted ligand-exchange recognition assay of glucose by quartz crystal microbalance," *Biosensors and Bioelectronics*, vol. 20, pp. 2197-2202, 2005.

[49] C. Wang, A. Javadi, M. Ghaffari, and S. Gong, "A pH-sensitive molecularly imprinted nanospheres/hydrogel composite as a coating for implantable biosensors," *Biomaterials*, vol. 31, pp. 4944-4951, 2010.